Atmos. Chem. Phys. Discuss., 13, 27597–27639, 2013
www.atmos-chem-phys-discuss.net/13/27597/2013/
doi:10.5194/acpd-13-27597-2013

Atmospheric Chemistry and Physics Discussions
Open Access

Estimating Asian terrestrial carbon fluxes from CONTRAIL aircraft and surface CO_2 observations for the period 2006 to 2010

H. F. Zhang[1,2], B. Z. Chen[1], I. T. van der Laan-Luijkx[3], T. Machida[4], H. Matsueda[5], Y. Sawa[5], Y. Fukuyama[6], C. Labuschagne[7], R. Langenfelds[8], M. van der Schoot[8], G. Xu[1,2], J. W. Yan[1,2], L. X. Zhou[9], P. P. Tans[10], and W. Peters[3,11]

[1]State Key Laboratory of Resources and Environment Information System, Institute of geographic Sciences and Natural Resources Research, Chinese Academy of Sciences, Beijing 100101, China
[2]University of Chinese Academy of Sciences, Beijing 100049, China
[3]Department of Meteorology and Air Quality (MAQ), Wageningen University, Droevendaalsesteeg 3a, 6700 PB, Wageningen, the Netherlands
[4]Center for Global Environmental Research, National Institute for Environmental Studies, Tsukuba, Japan
[5]Geochemical Research Department, Meteorological Research Institute, Tsukuba, Japan
[6]Atmospheric Environment Division, Global Environment and Marine Department, Japan Meteorological Agency, Japan
[7]South African Weather Service, P.O. Box 320, Stellenbosch, 7599, South Africa

[8]Centre for Australian Weather and Climate Research/CSIRO Marine and Atmospheric Research, Aspendale, Victoria, Australia
[9]Key Laboratory for Atmospheric Chemistry of China Meteorological Administration, Research Institute of Atmospheric Composition of Chinese Academy of Meteorological Sciences, Beijing 100081, China
[10]Earth System Research Laboratory, National Oceanographic and Atmospheric Administration, Boulder, Colorado 80305, USA
[11]Centre for Isotope Research, University of Groningen, Groningen, the Netherlands

Received: 9 October 2013 – Accepted: 11 October 2013 – Published: 24 October 2013

Correspondence to: B. Z. Chen (baozhang.chen@igsnrr.ac.cn)

Published by Copernicus Publications on behalf of the European Geosciences Union.

Abstract

Current estimates of the terrestrial carbon fluxes in Asia ("Asia" refers to lands as far west as the Urals and is divided into Boreal Eurasia, Temperate Eurasia and tropical Asia based on TransCom regions) show large uncertainties particularly in the boreal and mid-latitudes and in China. In this paper, we present an updated carbon flux estimate for Asia by introducing aircraft CO_2 measurements from the CONTRAIL (Comprehensive Observation Network for Trace gases by Airline) program into an inversion modeling system based on the CarbonTracker framework. We estimated the averaged annual total Asian terrestrial land CO_2 sink was about $-1.56\,\mathrm{Pg\,C\,yr^{-1}}$ over the period 2006–2010, which offsets about one-third of the fossil fuel emission from Asia ($+4.15\,\mathrm{Pg\,C\,yr^{-1}}$). The uncertainty of the terrestrial uptake estimate was derived from a set of sensitivity tests and ranged from -1.07 to $-1.80\,\mathrm{Pg\,C\,yr^{-1}}$, comparable to the formal Gaussian error of $\pm 1.18\,\mathrm{Pg\,C\,yr^{-1}}$ (1-sigma). The largest sink was found in forests, predominantly in coniferous forests ($-0.64\,\mathrm{Pg\,C\,yr^{-1}}$) and mixed forests ($-0.14\,\mathrm{Pg\,C\,yr^{-1}}$); and the second and third large carbon sinks were found in grass/shrub lands and crop lands, accounting for $-0.44\,\mathrm{Pg\,C\,yr^{-1}}$ and $-0.20\,\mathrm{Pg\,C\,yr^{-1}}$, respectively. The peak-to-peak amplitude of inter-annual variability (IAV) was $0.57\,\mathrm{Pg\,C\,yr^{-1}}$ ranging from $-1.71\,\mathrm{Pg\,C\,yr^{-1}}$ to $-2.28\,\mathrm{Pg\,C\,yr^{-1}}$. The IAV analysis reveals that the Asian CO_2 sink was sensitive to climate variations, with the lowest uptake in 2010 concurrent with summer flood/autumn drought and the largest CO_2 sink in 2009 owing to favorable temperature and plentiful precipitation conditions. We also found the inclusion of the CONTRAIL data in the inversion modeling system reduced the uncertainty by 11 % over the whole Asian region, with a large reduction in the southeast of Boreal Eurasia, southeast of Temperate Eurasia and most Tropical Asian areas.

ACPD
13, 27597–27639, 2013

1 Introduction

The concentration of carbon dioxide (CO_2) has been increasing steadily in the atmosphere since the industrial revolution, which is considered to be very likely responsible for the largest contribution of the climate warming (Huber and Knutti, 2011; Peters et al., 2011). Knowledge of the terrestrial carbon sources and sinks is critically important for understanding and projecting the future atmospheric CO_2 levels and climate change. The global terrestrial ecosystems absorbed about 1–3 Pg carbon every year during the 2000s, with obvious interannual variations, offsetting 10–40 % of the anthropogenic emissions (Le Quéré et al., 2009; Maki et al., 2010; Saeki et al., 2013). However, estimates of the terrestrial carbon balance vary considerably when considering continental scales and smaller, as well as when estimating the CO_2 seasonal and inter-annual variability (Houghton, 2007; Peylin et al., 2013).

Asia, as one of the biggest Northern Hemisphere terrestrial carbon sinks, has a significant impact on the global carbon budget (Jiang et al., 2013; Patra et al., 2012; Piao et al., 2009; Piao et al., 2012; Yu et al., 2013). It is estimated that Asian ecosystems contribute over 50 % of the global net terrestrial ecosystem exchange (Maksyutov et al., 2003) and their future balance is thought to be a great uncertainty source for the global carbon budget (Ichii et al., 2013; Oikawa and Ito, 2001). Even though the importance of the Asian ecosystems is increasingly recognized and many efforts have been carried out to estimate the Asian terrestrial carbon sources and sinks, they still remain poorly quantified (Ito, 2008; Patra et al., 2012, 2013; Piao et al., 2011). One reason is that many Asian countries have experienced rapid economic growth, steep population expansion and increasing energy demands, which have a large influence on the Asian carbon budget and has lead to an increased variability of the regional budget (Francey et al., 2013; Le Quere et al., 2009; Patra et al., 2011, 2013; Raupach et al., 2007). In addition, a big change in the regional land-use patterns as well as in the climate trends caused by global warming and climate variability have aggravated the uncertainty in the Asian terrestrial carbon balance (Cao et al., 2003; Patra et al., 2011; Yu et al., 2013). These human-induced disturbances and nature-induced variations in the terrestrial carbon flux together put a bigger challenge on accurately estimating CO_2 fluxes of the Asia ecosystems.

Currently two approaches are commonly used to estimate CO_2 fluxes at regional to global scales: the so-called "bottom-up" and "top-down" methods. The bottom-up approach is based on local data or field measurements to retrieve the carbon fluxes, including direct measurements (Chen et al., 2012; Clark et al., 2001; Fang et al., 2001; Mizoguchi et al., 2009; Takahashi et al., 1999) and ecosystem modeling (Chen et al., 2007; Fan et al., 2012; Randall et al., 1996; Randerson et al., 1997; Sellers et al., 1986, 1996). The top-down method uses atmospheric mole fraction data to derive the CO_2 sink/source information. As one of the important "top-down" approaches, atmospheric inversion modeling has been well developed and widely applied (Baker et al., 2006; Chevallier and O'Dell, 2013; Deng et al., 2007; Gurney et al., 2003, 2004), and has shown to be particularly successful in estimating regional carbon flux for regions rich in atmospheric CO_2 observations like North America and Europe (Broquet et al., 2013; Deng et al., 2007; Peters et al., 2007, 2010; Peylin et al., 2013, 2005; Rivier et al., 2011, 2010). However, estimating Asian CO_2 surface fluxes with inversion modeling remains challenging, and the inverted Asian CO_2 fluxes still exhibit a large uncertainty partly because of lack of surface CO_2 observations. For example, in the TransCom3 annual mean control inversion, Gurney et al. (2003) conducted a set of 17 models to estimate the carbon fluxes and obtained different results of Asian biosphere CO_2 budget with ranging from a large CO_2 source of $+1.00 \pm 0.61\,\mathrm{Pg\,C\,yr^{-1}}$ to a large sink of $-1.50 \pm 0.67\,\mathrm{Pg\,C\,yr^{-1}}$ for the year 1992–1996. In the RECCAP (REgional Carbon Cycle Assessment and Processes) project, Piao et al. (2012) presented the carbon balance of terrestrial ecosystems in East Asia from eight inversions during 1990–2009. The results from these eight inversion models also show disagreement: six models estimate a net CO_2 uptake with the highest net carbon sink of $-0.997\,\mathrm{Pg\,C\,yr^{-1}}$, while two models show a net CO_2 source with the largest net carbon emission of $+0.416\,\mathrm{Pg\,C\,yr^{-1}}$ in East Asia. The important role of the sparse observational network was demonstrated

ACPD
13, 27597–27639, 2013

by Maki et al. (2010), who reported a large Asian land sink of $-1.17 \pm 0.50\,\mathrm{Pg\,C\,yr^{-1}}$ or much smaller sink of $-0.65 \pm 0.49\,\mathrm{Pg\,C\,yr^{-1}}$ over the Asian region depending on which set of observations was included in the same inversion system. This situation suggests that a more accurate inverted estimate of the surface CO_2 flux is urgently required in Asia, and the ability to ingest as much observational data as possible is the key.

To expand the number of CO_2 observation data points, the aircraft project of CONTRAIL has been operated to measure CO_2 concentration onboard passenger flights since 2005, and has produced a large coverage of in situ CO_2 data ranging over various latitudes, longitudes, and altitudes (Machida et al., 2008; Matsueda et al., 2008). Huge amounts of CONTRAIL measurements have been measured and have already successfully been used to constrain surface flux estimates (Niwa et al., 2011, 2012; Patra et al., 2011). The latter paper shows the added value of CONTRAIL data to inform on tropical Asian carbon fluxes, as their signals are transported rapidly to the free troposphere over the West Pacific.

In this study, we also used the CONTRAIL CO_2 observations (http://www.cger.nies.go.jp/contrail/) together with a global network of surface observations to estimate the Asian weekly net ecosystem exchange of CO_2 (NEE) during the period 2006–2010. Our inversion model is the state-of-the-art CO_2 data assimilation system CTDAS (Carbon Tracker Data Assimilation Shell, http://carbontracker.eu/ctdas/). The approach is characterized by the following three components: (1) the atmospheric transport model TM5 (Krol et al., 2005) used as forward model in the data assimilation system was nested to a $1^\circ \times 1^\circ$ grid over Asia while globally it had a $2^\circ \times 3^\circ$ resolution (Fig. 1); (2) the number of surface CO_2 observation sites was expanded by including 14 sites in Asia; and (3) the CONTRAIL aircraft observations were introduced to the CTDAS atmospheric inversion system.

Our work complements previous inverse modeling studies as it: (1) presents the inverted CO_2 results of Asian weekly net ecosystem exchange not shown previously; (2) uses surface observations not available in an earlier top-down exercise; (3) assimilates the continuous CO_2 observation from a number of Asian continental sites for the first

ACPD
13, 27597–27639, 2013

time; (4) includes extra free tropospheric CO_2 observations to further constrain the estimate; (5) use a two-way atmospheric transport model with higher horizontal resolution than previous global CO_2 data assimilation studies that zoomed in Asia.

This paper is organized as follows. Methods and materials are described in Sect. 2, the inferred Asian land flux and its temporal-spatial variations are presented in Sect. 3. To examine the impact of CONTRAIL data on Asian flux estimation, we also compared inversion results with and without CONTRAIL data during 2006–2010. In Sect. 4, we compare our inverted Asian surface fluxes with previous findings and discuss our estimation uncertainty estimates and future directions. Note that the "Asia" refers to lands as far west as the Urals, and it is further divided into Boreal Eurasia, Temperate Eurasia and tropical Asia based on TransCom regions (Gurney et al., 2002, 2003) (see small inset in the bottom left corner of Fig. 2).

2 Methods and datasets

2.1 The atmospheric inversion model (CTDAS)

The atmospheric inversion model CTDAS developed by NOAA-ESRL (National Oceanic and Atmospheric Administration's Earth System Research Laboratory) & Wageningen University, the Netherlands. Previous versions of the system have been applied successfully in North America and Europe (Masarie et al., 2011; Peters et al., 2007, 2010). CTDAS was designed to estimate net CO_2 terrestrial and oceanic surface fluxes by integrating atmospheric CO_2 concentration measurements, a global transport model, and a Bayesian synthesis technique that minimizes the difference between the simulated and observed CO_2 concentrations. The first step is the forecast of the atmospheric CO_2 concentrations using the transport model TM5 (Krol et al., 2005) with a global resolution of $3^\circ \times 2^\circ$ and $1^\circ \times 1^\circ$ over Asia (see Fig. 1), driven by meteorological data of the European Centre for Medium-Range Weather Forecasts (ECMWF) and four separate sets of bottom-up fluxes (details are presented in the Sect. 2.2). Secondly,

ACPD
13, 27597–27639, 2013

these forecasted four-dimensional (4-D) concentrations (x,y,z,t) are sampled with the observed atmospheric CO_2 mole fractions at the location and time of the measurements, which are then compared. The difference between the observed and simulated CO_2 concentrations is minimized. This minimization of the concentration differences in CTDAS is done by tuning a set of linear scaling factors which are applied to find the set of sources and sinks that most closely match the observed CO_2 concentration in the atmosphere.

As described in Peters et al. (2007), four a-priori and imposed CO_2 fluxes integrate in CTDAS to instantaneous CO_2 fluxes $F(x,y,t)$ as follows:

$$F(x,y,t) = \lambda_r F_{\text{bio}}(x,y,t) + \lambda_r F_{\text{oce}}(x,y,t) + F_{\text{ff}}(x,y,t) + F_{\text{fire}}(x,y,t) \quad (1)$$

where F_{bio} and F_{oce} are 3 hourly, $1^{\circ} \times 1^{\circ}$ a-priori terrestrial biosphere and ocean fluxes, respectively; F_{ff} and F_{fire} are monthly $1^{\circ} \times 1^{\circ}$ prescribed fossil fuel and fire emissions, and λ_r is a set of weekly scaling factors, and each scaling factor is associated with a particular region of the global domain that is divided into 11 land and 30 ocean regions according to climate zone and continent. Nineteen ecosystem types (Olson et al., 1985) (Fig. 2a) have been considered in each of 11 global land areas (Gurney et al., 2002), dividing the global into 239 regions ($239 = 11$ land $\times$ 19 ecosystem types + 30 ocean regions). A set of weekly scaling factors were set to these regions. These scaling factors have been estimated as the final product of CTDAS, and have been applied to obtain the terrestrial biosphere and ocean fluxes at the ecosystem and ocean basin scale by multiplying them with the a-priori fluxes. The adjusted fluxes are then put into the transport model to produce an optimized 4-D CO_2 concentration distribution.

2.2 A priori CO_2 flux data set

In CTDAS, four types of CO_2 surface fluxes are considered: (1) the a-priori estimates of the oceanic CO_2 exchange are based on the air-sea CO_2 partial pressure differences from ocean inversions results (Jacobson et al., 2007), with the short-term flux variability derived from the atmospheric model wind speeds via the gas transfer coefficient. These

ACPD
13, 27597–27639, 2013

air-sea partial pressure differences are combined with a gas transfer velocity computed from wind speeds in the atmospheric transport model to compute fluxes of carbon dioxide across the sea surface every 3 h; (2) the a-priori terrestrial biosphere CO_2 fluxes are from the Carnegie–Ames Stanford Approach (CASA) biogeochemical model (Werf et al., 2006). A monthly varying NEE flux (NEE = R_e – GPP) was constructed from two flux components: gross primary production (GPP) and ecosystem respiration (R_e), and interpolated to 3 hourly net surface fluxes using a simple temperature Q_{10} relationship assuming a global Q_{10} value of 1.5 for respiration, and a linear scaling of photosynthesis with solar radiation. (3) The imposed fossil fuel emission estimates from the global total fossil fuel emission of the CDIAC (Carbon Dioxide Information and Analysis Center) (Marland et al., 2003) were spatially and temporally interpolated by the EDGAR (Emission Database for Global Atmospheric Research) database (Boden et al., 2011; EC-JRC/PBL, 2009; Olivier and Berdowski, 2001; Thoning et al., 1989); (4) the biomass burning emissions are from the GFED2 (Global Fire Emissions Database version 2), which combines monthly burned area information observed from satellites (Giglio et al., 2006) with the CASA biogeochemical model. Fire emissions in GFED2 are available only up to 2008, so for 2009 and 2010 we use a climatologically of monthly averages of the previous decade.

2.3 Atmospheric CO_2 observations

For this study, two sets of atmospheric CO_2 observation data were assimilated: (1) surface CO_2 observations distributed by NOAA-ESRL (http://www.esrl.noaa.gov/gmd/ccgg/obspack/) and by the WDCGG (World Data Centre for Greenhouse Gases, http://ds.data.jma.go.jp/gmd/wdcgg/) for the period 2006–2010 (see Fig. 2a). Individual time series in this surface set were provided by many individual PIs which we kindly acknowledge; (2) for the free tropospheric CO_2 observation, we use the aircraft measurements derived from the CONTRAIL project for the period 2006–2010 (see Fig. 2b).

A summary of Asian surface sites used in this study is shown in Table 1 and Fig. 2a for a reference. There are fourteen surface sites with over 7957 observations located in

ACPD
13, 27597–27639, 2013

Asia, of which 9 time series of CO_2 observations made by NOAA-ESRL [WLG and SDZ were also contributed from China Meteorological Administration (CMA)], one dataset (e.g. CRI) is provided by CSIRO (Commonwealth Scientific and Industrial Research Organization), one dataset (e.g. GSN) is made by the NIER (National Institute of Environmental Research, Republic of Korea) and the other three datasets (e.g. MNM, RYO, YON) are made by JMA (Japan Meteorological Agency). These surface CO_2 mole fraction data used in this study are all calibrated against the same CO_2 standard (WMO-X2007). For most of the continuous sampling sites at the surface, we derived a daily averaged afternoon CO_2 concentration (12:00–16:00 LT) for each day from the time series, while at mountain-top sites we construct an average based on nighttime hours (00:00–04:00 LT) to reduce local influence and compare modeled with observed values only for well mixed conditions.

In our assimilation system, we also use free tropospheric continuous aircraft measurements from the CONTRAIL program (Machida et al., 2008; Matsueda et al., 2008) to constrain the inverted CO_2 flux. Note that stratospheric CONTRAIL CO_2 data were not included into the CTDAS for the stratospheric observation had a seasonal phase shifting and its smaller amplitude was hard to comparable to the tropospheric data (Sawa et al., 2008). A summary of the CONTRAIL aircraft measurements is presented in Table 2 and Fig. 2b. The CONTRAIL aircraft data are reported on the NIES 09 CO_2 scale, which are lower than the WMO-X2007 CO_2 scale by 0.07 ppm at around 360 ppm and consistent in the range between 380 and 400 ppm (Machida et al., 2011). Thus the CONTRAIL CO_2 data sets are comparable to surface data well. We follow the method from Niwa et al. (2012) to divide the data into 4 vertical bins (575–625, 465–525, 375–425, 225–275 hPa) from ascending & descending profiles and one vertical bin (225–275 hPa) from leveling cruise. We also divide CONTRAIL data into 42 horizontal bins/regions (Fig. 2b), which amounts to a total of 65 bins corresponding to horizontal and vertical bins/regions. Before daily averaging the CONTRAIL measurements for each 65 regional/vertical bins, we pre-process the aircraft data to obtain free troposphere CO_2 values by filtering out of the stratospheric CO_2 data using the

ACPD
13, 27597–27639, 2013

threshold of potential vorticity (PV) > 2 PVU (1 PVU = 10^{-6} m^2 s^{-1} K kg^{-1}), in which PV is calculated from the TM5 (ECMWF temperature, pressure and wind fields) (Sawa et al., 2008). A total number of 10 467 CO_2 aircraft observations over Asia, which retrieved from the ascending, descending vertical profiles and the leveling cruise over the airports below 625 hPa during January 2006 to December 2010, have been used in our inversion.

2.4 Sensitivity experiments

Because the Gaussian uncertainties strongly depends on choices of prior errors in CTDAS, the formal covariance estimates for each week of optimization only reflect the random component of the particular problem rather than a characterization of the true uncertainties of the inverted CO_2 flux. As an alternative, we performed a set sensitivity experiments to obtain a more representative spread in the flux estimation and complement the formal Gaussian uncertainty estimates. We take different plausible alternative settings in CTDAS to design a comprehensive sensitivity tests, and use the minimum and maximum flux inferred in these experiments to present the range of the true flux we expected to be. Six inversions were performed to investigate the uncertainty span in this study:

Case 1: prior flux as in Sect. 2.2 + observation as in Sect. 2.3 + TM5 transport model runs at global 3° × 2° and a nested grid over Asia. This is the base simulation (surface-CONTRAIL) which performs the best assimilation on CO_2 source/sink and its results are used to analyze the 5 yr carbon balance in this study.

Case 2: same as Case 1, but excluding CONTRAIL Observations. We use these results (surface-only) to examine the impact of CONTRAIL data on Asian flux estimates by comparing with Case 1.

Case 3: Like Case 1, but CTDAS runs with the updated fossil fuel emissions based on Wang et al. (2012) over China; This simulation is meant to partly address the impact

ACPD
13, 27597–27639, 2013

of uncertainty in fossil fuel emissions over the region as suggested by Francey et al. (2013).

Case 4: Like Case 1, but CTDAS runs based on 110 % of prior biosphere flux derived from CASA.

Case 5: Like Case 2, but the TM5 transport model is used at global 6° × 4° without nested grids. This tests the impact of model resolutions.

Case 6: Like case 2, but replacing the underlying land use map with MODIS data (Friedl et al., 2002) and keeping the number of ecoregions unchanged.

The Cases 1 and 2 span the period 2006–2010, while the other sensitivity experiments were done from 2008 to 2010 only when the observational coverage was best. In generally, the simulations of these 6 sensitivity tests investigate most variations in the components of the assimilation framework: prior fluxes, observation available, ecoregion map, fossil fuel emissions and transport. The results are summarized in the Table 3 and further discussed in the next Section.

3 Results

We will from here on refer to carbon sinks with a negative sign, source with a positive, and will include the sign also when discussing anomalies (positive = less uptake or larger source, negative = more uptake or smaller source).

3.1 CO_2 simulations

First we check the accuracy of the optimized model simulation using the surface CO_2 observations and the CONTRAIL aircraft CO_2 measurements. Figure 3a compares modeled CO_2 concentration with measurements at the surface site of MNM (see detailed information in Table 1). The comparison of the surface CO_2 time series shows that the simulated CO_2 concentrations is in good agreement with observed data during the period 2006–2010. The observed amplitudes in the CO_2 concentration are repro-

ACPD
13, 27597–27639, 2013

duced well, and the seasonal variations show accurate timing in spring (March–April–May) and autumn (September–October–November) but sometimes with weaker amplitudes in winter (December–January–February) and summer (June–July–August). This mismatch in CO_2 seasonal amplitude suggests that our estimated CO_2 surface fluxes do not catch the peak of terrestrial carbon uptake and emissions in summer and winter. Previous studies have also found this seasonal mismatch, which may correlate with atmospheric transport, and has already been identified as a shortcoming in most inversions (Peylin et al., 2013; Stephens et al., 2007; Yang et al., 2007). Figure 3b and c shows the histogram of residual distribution (simulated minus observed) in summer and winter. At MNM, the annual mean bias is $+0.15 \pm 0.87$ ppm ($+0.21 \pm 0.90$ ppm without CONTRAIL data), with a relatively large model overestimate of $+0.51 \pm 0.93$ ppm ($+0.58 \pm 1.03$ ppm without CONTRAIL data) in summer and a small bias of -0.05 ± 0.89 ppm ($+0.06 \pm 0.84$ ppm without CONTRAIL data) in winter. When considering all sites, the simulated mole fractions exhibit good agreement with the observed CO_2 time series and the change in inferred mixing ratios and flux are within the specified uncertainties in our inversion system, an important prerequisite for a good flux estimate.

We also check the model performance in the free troposphere in addition to the surface CO_2. Figure 3d shows the comparison between CO_2 measurements in the free troposphere during the period 2006–2010 in the region covering 136–144° N, 32–40° E, 375–425 hPa. The simulated troposphere CO_2 concentration also matches the CONTRAIL measurements well. Similar to the surface CO_2, we find seasonal mismatches in the summer and winter (Fig. 3e and f). The relatively small annual mean of model bias (model-minus-observed) in the free troposphere (-0.01 ± 1.18 ppm) is an integrated result of an overestimate ($+0.35 \pm 1.2$ ppm) in summer and an underestimate (-0.29 ± 0.99 ppm) in winter. Overall, the agreement between model and measurement for both the surface and CONTRAIL observations is fairly good and consistent with previously known behavior in the CarbonTracker systems, derived then mostly from North American and European continuous sites. Most importantly, residuals and innovation

ACPD
13, 27597–27639, 2013

Title Page
Abstract | Introduction
Conclusions | References
Tables | Figures
◀| |▶
◀ ▶
Back | Close
Full Screen / Esc
Printer-friendly Version
Interactive Discussion

statistics (not shown) suggests that our inverted fluxes, 26 470 CO_2 observations (7957 surface observations; 10 467 CONTRAIL observations), and simulated horizontal and vertical transport in CTDAS are to a high degree consistent with each other over Asia.

3.2 Inversed Asian terrestrial CO_2 flux

3.2.1 Five-year mean

During the period 2006–2010, we found a mean net terrestrial carbon uptake in Asia of $-1.56\,\mathrm{Pg\,C\,yr^{-1}}$ ($-1.09\,\mathrm{Pg\,C\,yr^{-1}}$ without CONTRAIL data), consisting of $-2.02\,\mathrm{Pg\,C\,yr^{-1}}$ ($-1.56\,\mathrm{Pg\,C\,yr^{-1}}$ without CONTRAIL data) uptake by the terrestrial biosphere and $+0.47\,\mathrm{Pg\,C\,yr^{-1}}$ release by biomass burning. This terrestrial uptake partly compensates the CO_2 emissions from fossil fuel burning and cement manufacturing of $+4.15\,\mathrm{Pg\,C\,yr^{-1}}$. An uncertainty for the Asian terrestrial CO_2 uptake derived from a set of sensitivity experiments has been conducted and the estimated sink ranges from -1.07 to $-1.80\,\mathrm{Pg\,C\,yr^{-1}}$, while the formal Gaussian uncertainty estimates are $-1.56 \pm 1.18\,\mathrm{Pg\,C\,yr^{-1}}$ retrieved from the posterior covariance. The estimated Asian net terrestrial CO_2 sink is further partitioned into 65 % of the carbon sinks in Boreal Eurasia ($-1.02\,\mathrm{Pg\,C\,yr^{-1}}$) and 44 % in Temperate Eurasia ($-0.68\,\mathrm{Pg\,C\,yr^{-1}}$), whereas 9 % release of CO_2 from the tropical Asia ($+0.14\,\mathrm{Pg\,C\,yr^{-1}}$).

The annual mean spatial distribution of net terrestrial carbon uptake over Asia is shown in Fig. 4. Note that the estimated fluxes include terrestrial fluxes and biomass burning sources but exclude fossil fuel emissions. Most Asian regions were natural carbon sinks over the studied period, with strongest carbon uptake in the middle and high latitudes of the Northern Hemispheric part of Asia, while the low-latitude region releases CO_2 to the atmosphere. This flux distribution pattern is quite consistent with previous findings that northern temperate and high latitude ecosystems were large sinks (Hayes et al., 2011) and tropical land was carbon sources (Gurney et al., 2003).

The aggregated terrestrial CO_2 fluxes for 19 different ecosystems (Fig. 2a) averaged over the period 2006–2010 are shown in Table 4 and Fig. 5 (see Case 1). The

ACPD
13, 27597–27639, 2013

majority of the carbon sink was found in the regions dominated by forests, crops and grass/shrubs. The largest uptake is by the forests with a mean sink of $-0.77\,\mathrm{Pg\,C\,yr^{-1}}$ (49 % of the total Asian fluxes), 41 % of which ($-0.64\,\mathrm{Pg\,C\,yr^{-1}}$) was taken up by conifer forests and 9 % of which ($-0.14\,\mathrm{Pg\,C\,yr^{-1}}$) by mixed forest, whereas the tropical forests released CO_2 by the amount of $+0.08\,\mathrm{Pg\,C\,yr^{-1}}$. The estimated flux by CTDAS in the Asian cropland ecosystems was $-0.20\,\mathrm{Pg\,C\,yr^{-1}}$, with the largest crop carbon sink located in Temperate Eurasia ($-0.17\,\mathrm{Pg\,C\,yr^{-1}}$). The grass/shrub lands in Asia absorbed $-0.44\,\mathrm{Pg\,C\,yr^{-1}}$, with most of these grass/shrub sinks located in Temperate Eurasia ($-0.36\,\mathrm{Pg\,C\,yr^{-1}}$). Other land-cover types (e.g. wetland, semi tundra and so on) sequestered about $-0.15\,\mathrm{Pg\,C\,yr^{-1}}$ (10 % of total) over Asian areas. This suggests that according to our model, many ecosystems contributed to AsianCO_2 sinks, highlighting a complexity of the northern hemispheric total sinks.

3.2.2 Interannual variability (IAV)

Figure 6 shows the estimated annual cumulative net ecosystem exchange in Asia during 2006–2010 as well as its anomaly with weekly intervals based on Case 2 (surface-only). Here, the biomass burning and fossil fuel emissions are excluded, and only the fluxes from respiration and photosynthesis are shown, because biomass burning emissions have large interannual variability, especially for Tropical Asia.

The coefficient of IAV (IAV = standard deviation/mean) in Asian land carbon flux is 0.12, with a peak-to-peak amplitude of $0.57\,\mathrm{Pg\,C\,yr^{-1}}$ (amplitude = smallest – largest CO_2 sink), ranging from the smallest carbon uptake of $-1.71\,\mathrm{Pg\,C\,yr^{-1}}$ in 2010 and the largest CO_2 sink of $-2.28\,\mathrm{Pg\,C\,yr^{-1}}$ in 2009. As has been noted in many other studies (Gurney et al., 2004, 2008; Mohammat et al., 2012; Patra et al., 2011; Peters et al., 2007, 2010; Valsala et al., 2013; Yu et al., 2013), the IAV of the carbon flux strongly correlates with climate factors, such as air temperature, precipitation and moistures.

The year 2010 stands out as a particularly low uptake year in Asia, with a reduction of terrestrial uptake estimated of $+0.31\,\mathrm{Pg\,C\,yr^{-1}}$ compared to the five-year mean.

ACPD
13, 27597–27639, 2013

This reduction phenomenon mainly appeared in Temperate Eurasia and Tropical Asia, leading to a $+0.25\,\mathrm{Pg\,C\,yr^{-1}}$ (35 % reduction) and $+0.04\,\mathrm{Pg\,C\,yr^{-1}}$ flux anomaly (24 % reduction) in their Corresponding regions. In 2010, Asia experienced a set of anomaly climate events. For example, Temperate Eurasia experienced a severe spring/autumn drought, a heavy summer flood and a heat wave occurred in 2010 (NationalClimateCenter, 2011). From Fig. 6b, we can see that 2010 did not appear largely anomalous followed by a spring growing season. As anomalous climate appeared, the summer flood and autumn drought were identified as dominant climatic factors controlling vegetation growth and exhibiting a significant correlation with the land carbon sink, particularly in the croplands, grasslands and forests of Temperate Eurasia. Finally, 2010 only ingested $-1.71\,\mathrm{Pg\,C\,yr^{-1}}$ CO_2 flux at the end of the year.

In contrast to 2010, the year of 2009 had the strongest carbon sink for the study period, with much stronger uptake in Temperate Eurasia ($-0.20\,\mathrm{Pg\,C\,yr^{-1}}$ anomaly, 28 % increase in CO_2 uptake) as well as Boreal Eurasia ($-0.05\,\mathrm{Pg\,C\,yr^{-1}}$ anomaly, 4 % uptake increase compared to the five-year mean). It can be seen that 2009 started with a lower-than-average release of carbon in the first 4 months (17 weeks) of the year amounting to $+0.28\,\mathrm{Pg\,C\,yr^{-1}}$ compared to the five-year average of $+0.45\,\mathrm{Pg\,C\,yr^{-1}}$. This variation of the Asian terrestrial carbon sink in the spring vegetation growing season may partly relate to a higher spring temperature in 2009 which induced an earlier onset of the growing season and lead to a high vegetation productivity by extending the growing season (Mohammat et al., 2012; Richardson et al., 2009; Walther et al., 2002; Wang et al., 2011; Yu et al., 2013). From Fig. 6b, 2010 shows a very high carbon uptake in the summer growing season (June–August, week 22 to 32) concurrent with favorable temperature and abundant precipitation conditions. After this summer, the vegetation productivity returned back to normal and the total cumulative carbon sink added up to $-2.28\,\mathrm{Pg\,C\,yr^{-1}}$ at the end of the year with $-0.26\,\mathrm{Pg\,C\,yr^{-1}}$ extra uptake compared to the five-year mean.

ACPD
13, 27597–27639, 2013

3.2.3 Uncertainty estimation

Table 3 presents the estimated annual mean NEE across the alternative sensitivity experiments. The alternative in CO_2 uptake ranges from -1.07 to $-1.80\,\mathrm{Pg\,C\,yr^{-1}}$ across our sensitivity experiments, which complements the Gaussian error. Despite the small numbers of years included, this range suggests that the Asian terrestrial was a sizable sink, while a carbon source in previous studies implied by the 1-sigma Gaussian error of $\pm 1.18\,\mathrm{Pg\,C\,yr^{-1}}$ on the estimated mean, is very unlikely. The largest sensitivity in inferred flux is to the change of land cover types (Case 6) and to the variations in prior terrestrial biosphere fluxes (Case 4). The inversion with updated Chinese fossil fuel emissions (Case 3) also shows the large variations in the inverted CO_2 flux, while the sensitivity to the TM5 model resolution (Case 5) is generally modest.

3.2.4 Impacts of the CONTRAIL data on inverted Asian CO_2 flux

We examined the impacts of the CONTRAIL data on Asian flux estimation by comparing results from Case 1 (surface-CONTRAIL) and Case 2 (surface-only) (Table 5 and Fig. 7a). Note that the uncertainties shown in the Table 5 and Fig. 7b are now the Gaussian uncertainties as we did not repeat all sensitivity experiments for Case 2. Inclusion of the CONTRAIL data induces an averaged extra CO_2 sink of about $-0.47\,\mathrm{Pg\,C\,yr^{-1}}$, with most of which adding in the grass/shrub ecosystem (Fig. 5). The spatial pattern of Asian fluxes also changed considerably (see Fig. 7a). For instance, a decrease in CO_2 uptake was found in the north area of Boreal Eurasia while an increase in the south of Boreal Eurasia, leading to an almost identical total carbon sink strength in the Boreal Asia between with and without CONTRAIL data. Whereas the estimated flux distribution in the Tropical Asia showed a small spatial change and a large increase in regional sink size with CONTRAIL observations.

Figure 7b shows the reduction of Gaussian error between Case 1 and Case 2. The error reduction rate (ER) is calculated as a percentage:

$$\mathrm{ER} = (\sigma_{\text{surface-only}} - \sigma_{\text{surface-CONTRAIL}})/\sigma_{\text{surface-only}} \times 100. \quad (2)$$

ACPD
13, 27597–27639, 2013

Where $\sigma_{\text{surface-only}}$ and $\sigma_{\text{surface-CONTRAIL}}$ are Gaussian errors in Case 2 (surface-only) and Case 1 (surface-CONTRAIL), respectively. By including the additional CONTRAIL data into the inversion system, the uncertainty of the posterior flux over Asia is significantly reduced (> 10 %), especially for the southeast of Boreal Eurasia, southeast of Temperate Eurasia and Tropical areas (up to 20–30 %). A more pronounced reduction was found in Boreal Eurasia and Tropical Asia (reducing by 14 % and 15 %, respectively). This suggests that current surface CO_2 observations data alone do not sufficiently constrain these regional flux estimation (there are no observations sites in the Boreal Eurasia and only one in the Tropical Asia), and the additional CONTRAIL CO_2 observations impose an extra constraint that can help reduce uncertainty on inferred Asia CO_2 flux, especially for these two surface observation lacked regions. We also found the error reduction in Temperate Eurasia is relatively small (< 10 %), especially for the west of Temperate Eurasia (< 1 %) because of a relative abundance of surface CO_2 observations in this region.

4 Discussions and conclusions

4.1 Impact of CONTRAIL

Our modeling experiments reveal that the extra aircraft observation data shift the inverted CO_2 flux estimates by imposing further constraints. This confirms the earlier findings by Saeki et al. (2003) and Maksyutov et al. (2013) that the inverted fluxes were sensitivity to observation data used. For Tropical Asia, inclusion of the CONTRAIL data notably reduced the uncertainties (about 15 % reduction). Compared with an inversion study with the CONTRAIL data for the Tropical Asia region (Niwa et al., 2012), the error reduction rate in land flux estimation in this study (15 %) for the same region is smaller than that of Niwa et al. (34 %). This difference in uncertainty reductions is likely the result of many differences in system design between the two studies, of which the assigned covariance to observations and prior fluxes is typically most important. We furthermore note that the set of observations used in these studies was not identical, we for instance included one tropical surface site (BKT, see Table 1 and Fig. 2a) to constrain the inferred flux estimation but Niwa et al. (2012) did not.

Our results share other features with the Niwa et al. (2012) study, for instance the relatively largest impact on the least data constrained regions. Reported by Niwa et al. (2012), the inclusion of CONTRAIL measurements not only constrains the underneath or nearby fluxes, but also reduces inferred flux errors in the regions far from the CONTRAIL measurement locations. For instance, in Boreal Eurasia, where no surface site exists and which is far from the CONTRAIL data locations (after pre-processing of horizontal/vertical bins and filter operation of stratospheric, there is no any CONTRAIL observation available over this region), uncertainty reductions are large (14 % reduction in uncertainty). Similar results were also presented by Niwa et al. (2012), with an 18 % error reduction in Boreal Eurasia. These two studies consistently suggest that including the CONTRAIL measurements in inversion modeling systems will help to increase the NEE estimation accuracy over Boreal Eurasia.

The CONTRAIL contribution to Temperate Eurasia is generally modest, only having a 6 % error reduction. This may due to that Temperate Eurasia has more surface observation sites than other regions in Asia. However, it is interesting that the difference in inverted NEE in this region between surface-only and surface-CONTRAIL are large ($-0.35\,PgC\,yr^{-1}$), but inconsistent with Niwa et al. (2012). One cause of this is likely the sensitivity of these inverse systems to vertical transport (Stephens et al., 2007), as also suggested by Niwa et al. (2012). The uneven distribution of observations at the surface and free troposphere may also aggravate this discrepancy.

4.2 Comparison of the estimated Asian CO_2 flux with other studies

Our estimated Asian terrestrial carbon sink is about $-1.56\,PgC\,yr^{-1}$ for the period 2006–2010. Most parts of Asian were estimated to be CO_2 sinks, with the largest carbon sink ($-1.02\,PgC\,yr^{-1}$) in Boreal Eurasia, a second large CO_2 sink ($-0.68\,PgC\,yr^{-1}$)

ACPD
13, 27597–27639, 2013

in Temperate Eurasia, while a small source ($+0.15\,\mathrm{Pg\,C\,yr^{-1}}$) in Tropical Asia. This distributions of estimated terrestrial CO_2 fluxes are overall comparable to the results for the period of 2000 to 2009 by Saeki et al. (2013), derived from an inversion approach focusing on Siberia with additional Siberian aircraft and tower CO_2 measurements, especially in the high latitude areas.

Comparisons of our inverted CO_2 flux with previous studies are summarized in Table 6. In Boreal Eurasia, our inferred land flux ($-1.02\,\mathrm{Pg\,C\,yr^{-1}}$) is in the range of Maki et al. (2010) ($-1.46\,\mathrm{Pg\,C\,yr^{-1}}$ from CNTL experiments, $-1.38\,\mathrm{Pg\,C\,yr^{-1}}$ from OBS experiments) and Gurney et al. (2003) ($-0.59\,\mathrm{Pg\,C\,yr^{-1}}$). In Temperate Eurasia, our inverted flux is $-0.68\,\mathrm{Pg\,C\,yr^{-1}}$, which is higher than that reported by Piao et al. (2012) ($-0.38\,\mathrm{Pg\,C\,yr^{-1}}$) and Maki et al. (2010) ($+0.96\,\mathrm{Pg\,C\,yr^{-1}}$ from CNTL experiments, $+0.37\,\mathrm{Pg\,C\,yr^{-1}}$ from OBS experiments), but is close to Gurney et al. (2003) ($-0.60\,\mathrm{Pg\,C\,yr^{-1}}$). In Tropical Asia, our estimate is $+0.15\,\mathrm{Pg\,C\,yr^{-1}}$, which is in the range of Niwa et al. (2012) ($+0.45\,\mathrm{Pg\,C\,yr^{-1}}$) and Patra et al. (2013) ($-0.104\,\mathrm{Pg\,C\,yr^{-1}}$), both including aircraft CO_2 measurements in their inversion modeling. Our estimate of the total Asian terrestrial carbon sink ($-1.56\,\mathrm{Pg\,C\,yr^{-1}}$) is close to the findings by Maki et al. (2010) of $-1.17\,\mathrm{Pg\,C\,yr^{-1}}$ derived from OBS experiments during 2001 to 2007, but much higher than the results of Gurney et al. (2003) ($-0.52\,\mathrm{Pg\,C\,yr^{-1}}$) for the period of 1992 to 1996. Compared to the previous findings, our updated Asia NEE estimation seems to support a large Asian carbon sink over the past decade.

The spatial patterns of NEE in Asia are complex because of large land surface heterogeneity, such as land cover, vegetation growth, soil types, etc. In addition, climate change and land use change and human activities impose on seasonal and interannual changes in NEE. All these factors make that to accurately estimate NEE over Asia area is a big challenge. We believe this study is therefore useful to improve our understanding of the Asia regional terrestrial carbon cycle processes even though our estimation still exhibit considerable uncertainties and biases in the inverted fluxes due to data availability and limited methodology. By these comparisons, we can also conclude that our inferred Asia land surface CO_2 fluxes support a view that both large

ACPD
13, 27597–27639, 2013

boreal and mid-latitude carbon sinks in Asian balanced partly a small tropical source. This would support the earlier suggestion that the Asia region is of key interest to better understand the global terrestrial carbon budget in the context of climate change.

The majority of the CO_2 sink was found in the areas dominated by forests, crops and grass/shrubs. Asian forests were estimated to be a large sink ($-0.77\,\mathrm{Pg\,C\,yr^{-1}}$) during 2006–2010, the sink size is slightly larger than the bottom-up derived results of Pan et al. (2011) ($-0.62\,\mathrm{Pg\,C\,yr^{-1}}$) for the period 1990–2007. One cause of this discrepancy is likely due to that our estimate is presented at a coarse resolution (a $1^{\circ} \times 1^{\circ}$ grid may contain other biomes with low carbon uptake than forests). Another reason may be that about half of the Temperate Eurasia was not included in the statistical analysis by Pan et al. (2011). Note that the carbon accumulation in wood products is not considered in our estimates and needs further analysis in future studies.

The croplands in Asia were identified to be an average sink of $-0.20\,\mathrm{Pg\,C\,yr^{-1}}$ during 2006–2010, which is consistent with the previous findings by Chen et al. (2013). The uptake in croplands is likely associated with agricultural technique and cropping management. Different from other natural ecosystems, crop ecosystems are usually under intensive farming cultivation, with regular fertilizing and irrigation of the crops according to plants growing properties. These cultivation practice increases the crop production, and in return lead to high residues and root to the soil, which largely increase the carbon sink in cropland (Chen et al., 2013). However, the accumulation of crop carbon in most crop ecosystems is relatively low, in which agricultural areas are even considered no contribution to a long-term net sink (Fang et al., 2007; Piao et al., 2009; Tian et al., 2011). This is because the carbon accumulation in the crop biomass is harvested at least once per year and released back as CO_2 to the atmosphere. We should note that our estimate in the crop sink is different from the results of "crop no contribution" (Piao et al., 2009). Our atmospheric inversion system can well capture the crop's strong CO_2 uptake during growing season, but the atmosphere locally does not reflect the emission of the harvested crops, which normally has been transported laterally and is consumed elsewhere. This harvested product is likely released from a region with high population density and hard to detect against high fossil fuel emissions, whereas the estimated crop flux remains a large net CO_2 uptake over the period considered even though the crop flux into the soil is relatively small. This issue was also raised by Peters et al. (2007, 2010).

Grassland/Shrub ecosystems also play an important role in the global carbon cycle, accounting for about 20 % of total terrestrial production and could be a potential carbon sink in future (Scurlock and Hall, 1998). The grass/shrub lands in Asia absorb CO_2 of $-0.44\,\mathrm{Pg\,C\,yr^{-1}}$, accounting for about 25 % of the total Asian terrestrial CO_2 sink, which is close to the averaged global grassland sink percentage of 20 %. Compared to the bottom-up results that net ecosystem productivity was $10.18\,\mathrm{g\,C\,m^{-2}\,yr^{-1}}$ by Yu et al. (2013), our estimate of $34.32\,\mathrm{g\,C\,m^{-2}\,yr^{-1}}$ is much higher. This might due to that the areas in this study include shrubs whereas other studies only considering grass lands.

Acknowledgements. We wish to thank the Y. Niwa of Geochemical Research Department, Meteorological Research Institute, Tsukuba, Japan for providing many important comparable results and useful comments on this study. We kindly acknowledge all atmospheric data providers to the NOAA Cooperative Air Sampling network, and those that contribute their data to WDCGG. We are grateful to Michel Ramonet of French RAMCES (Réseau Atmosphérique de Mesure des Composés à Effet de Serre), Angel J. Gomez-Pelaez of Izaña Atmospheric Research Center (IARC), Meteorological State Agency of Spain (AEMET), Spain, Britt Stephens of NCAR, Laszlo Haszpra of Hungarian Meteorological Service and Samuel Hammer of University of Heidelberg, Institut fuer Umweltphysik for CO_2 time series used in this assimilation system. This research is supported by the Strategic Priority Research Program "Climate Change: Carbon Budget and Related Issues" of the Chinese Academy of Sciences (Grant nr. XDA05040403), the National High Technology Research and Development Program of China (Grant no. 2013AA122002), the research grants (41071059 & 41271116) funded by the National Science Foundation of China, a Research Plan of LREIS (O88RA900KA), CAS, a research grant (2012ZD010) of Key Project for the Strategic Science Plan in IGSNRR, CAS, and "One Hundred Talents" program funded by the Chinese Academy of Sciences. Wouter Peters was supported by an NWO VIDI Grant (864.08.012) and the Chinese–Dutch collaboration was funded by the China Exchange Program project (12CDP006). I. van der Laan-Luijkx has received funding from the European Union's Seventh Framework Programme (FP7/2007–2013) under grant agreement n° 283080, project GEOCARBON.

References

Baker, D., Law, R., Gurney, K., Rayner, P., Peylin, P., Denning, A., Bousquet, P., Bruhwiler, L., Chen, Y. H., and Ciais, P.: TransCom 3 inversion intercomparison: impact of transport model errors on the interannual variability of regional CO_2 fluxes, 1988–2003, Global Biogeochem. Cy., 20, GB1002, doi:10.1029/2004GB002439, 2006.

Boden, T., Marland, G., and Andres, R.: Global, regional, and national fossil-fuel CO_2 emissions, Carbon Dioxide Information Analysis Center, Oak Ridge National Laboratory, US Department of Energy, Oak Ridge, TN, USA, doi:10.3334/CDIAC/00001_V2011, 10 pp., 2011.

Broquet, G., Chevallier, F., Bréon, F.-M., Kadygrov, N., Alemanno, M., Apadula, F., Hammer, S., Haszpra, L., Meinhardt, F., Morguí, J. A., Necki, J., Piacentino, S., Ramonet, M., Schmidt, M., Thompson, R. L., Vermeulen, A. T., Yver, C., and Ciais, P.: Regional inversion of CO_2 ecosystem fluxes from atmospheric measurements: reliability of the uncertainty estimates, Atmos. Chem. Phys., 13, 9039–9056, doi:10.5194/acp-13-9039-2013, 2013.

Cao, M., Prince, S. D., Li, K., Tao, B., Small, J., and Shao, X.: Response of terrestrial carbon uptake to climate interannual variability in China, Glob. Change Biol., 9, 536–546, 2003.

Chen, B., Chen, J. M., and Ju, W.: Remote sensing-based ecosystem–atmosphere simulation scheme (EASS) – Model formulation and test with multiple-year data, Ecol. Model., 209, 277–300, 2007.

Chen, B., Coops, N. C., Fu, D., Margolis, H. A., Amiro, B. D., Black, T. A., Arain, M. A., Barr, A. G., Bourque, C. P. A., and Flanagan, L. B.: Characterizing spatial representativeness of flux tower eddy-covariance measurements across the Canadian Carbon Program Network using remote sensing and footprint analysis, Remote Sens. Environ., 124, 742–755, 2012.

Chen, Z., Yu, G., Ge, J., Sun, X., Hirano, T., Saigusa, N., Wang, Q., Zhu, X., Zhang, Y., and Zhang, J.: Temperature and precipitation control of the spatial variation of terrestrial ecosystem carbon exchange in the Asian region, Agr. Forest Meteorol., 182–183, 266–276, 2013.

Chevallier, F. and O'Dell, C. W.: Error statistics of Bayesian CO_2 flux inversion schemes as seen from GOSAT, Geophys. Res. Lett., 40, 1252–1256, 2013.

Clark, D. A., Brown, S., Kicklighter, D. W., Chambers, J. Q., Thomlinson, J. R., and Ni, J.: Measuring net primary production in forests: concepts and field methods, Ecol. Appl., 11, 356–370, 2001.
EC-JRC/PBL: European Commission: Joint Research Centre (JRC)/Netherlands Environmental Assessment Agency (PBL): Emission Database for Global Atmospheric Research (EDGAR), release version 4.0, http://edgar.jrc.ec.europa.eu, 2009.
Deng, F., Chen, J. M., Ishizawa, M., Yuen, C. W. A. I., Mo, G., Higuchi, K., Chan, D., and Maksyutov, S.: Global monthly CO_2 flux inversion with a focus over North America, Tellus B, 59, 179–190, 2007.
Fan, Z. M., Li, J., and Yue, T. X.: Changes of climate–vegetation ecosystem in loess plateau of China, Procedia Environmental Sciences, 13, 715–720, 2012.
Fang, J., Chen, A., Peng, C., Zhao, S., and Ci, L.: Changes in forest biomass carbon storage in China between 1949 and 1998, Science, 292, 2320–2322, 2001.
Fang, J., Guo, Z., Piao, S., and Chen, A.: Terrestrial vegetation carbon sinks in China, 1981–2000, Sci. China Ser. D, 50, 1341–1350, 2007.
Francey, R. J., Trudinger, C. M., van der Schoot, M., Law, R. M., Krummel, P. B., Langenfelds, R. L., Steele, L. P., Allison, C. E., Stavert, A. R., and Andres, R. J.: Atmospheric verification of anthropogenic CO_2 emission trends, Nature Climate Change, 3, 520–524, 2013.
Friedl, M. A., McIver, D. K., Hodges, J. C., Zhang, X., Muchoney, D., Strahler, A. H., Woodcock, C. E., Gopal, S., Schneider, A., and Cooper, A.: Global land cover mapping from MODIS: algorithms and early results, Remote Sens. Environ., 83, 287–302, 2002.
Giglio, L., van der Werf, G. R., Randerson, J. T., Collatz, G. J., and Kasibhatla, P.: Global estimation of burned area using MODIS active fire observations, Atmos. Chem. Phys., 6, 957–974, doi:10.5194/acp-6-957-2006, 2006.
Gurney, K. R., Law, R. M., Denning, A. S., Rayner, P. J., Baker, D., Bousquet, P., Bruhwiler, L., Chen, Y. H., Ciais, P., and Fan, S.: Towards robust regional estimates of CO_2 sources and sinks using atmospheric transport models, Nature, 415, 626–630, 2002.
Gurney, K. R., Law, R. M., Denning, A. S., Rayner, P. J., Baker, D., Bousquet, P., Bruhwiler, L., Chen, Y. H., Ciais, P., and Fan, S.: TransCom 3 CO_2 inversion intercomparison: 1. annual mean control results and sensitivity to transport and prior flux information, Tellus B, 55, 555–579, 2003.
Gurney, K. R., Law, R. M., Denning, A. S., Rayner, P. J., Pak, B. C., Baker, D., Bousquet, P., Bruhwiler, L., Chen, Y. H., and Ciais, P.: Transcom 3 inversion intercomparison: model mean

results for the estimation of seasonal carbon sources and sinks, Global Biogeochem. Cy., 18, GB1010, doi:10.1029/2003GB002111, 2004.
Gurney, K. R., Baker, D., Rayner, P., and Denning, S.: Interannual variations in continental-scale net carbon exchange and sensitivity to observing networks estimated from atmospheric CO_2 inversions for the period 1980 to 2005, Global Biogeochem. Cy., 22, GB3025, doi:10.1029/2007GB003082, 2008.
Hayes, D. J., McGuire, A. D., Kicklighter, D. W., Gurney, K. R., Burnside, T., and Melillo, J. M.: Is the northern high-latitude land-based CO_2 sink weakening?, Global Biogeochem Cy, 25, GB3018, doi:10.1029/2010GB003813, 2011.
Houghton, R.: Balancing the global carbon budget, Annu. Rev. Earth Pl. Sc., 35, 313–347, 2007.
Huber, M. and Knutti, R.: Anthropogenic and natural warming inferred from changes in Earth's energy balance, Nat. Geosci., 5, 31–36, 2011.
Ichii, K., Kondo, M., Lee, Y.-H., Wang, S.-Q., Kim, J., Ueyama, M., Lim, H.-J., Shi, H., Suzuki, T., and Ito, A.: Site-level model-data synthesis of terrestrial carbon fluxes in the CarboEastAsia eddy-covariance observation network: toward future modeling efforts, J. Forest Res.-Jpn., 18, 13–20, 2013.
Ito, A.: The regional carbon budget of East Asia simulated with a terrestrial ecosystem model and validated using AsiaFlux data, Agr. Forest Meteorol., 148, 738–747, 2008.
Jacobson, A. R., Mikaloff Fletcher, S. E., Gruber, N., Sarmiento, J. L., and Gloor, M.: A joint atmosphere–ocean inversion for surface fluxes of carbon dioxide: 1. methods and global-scale fluxes, Global Biogeochem. Cy., 21, GB1020, doi:10.1029/2006GB002703, 2007.
Jiang, F., Wang, H. W., Chen, J. M., Zhou, L. X., Ju, W. M., Ding, A. J., Liu, L. X., and Peters, W.: Nested atmospheric inversion for the terrestrial carbon sources and sinks in China, Biogeosciences, 10, 5311–5324, doi:10.5194/bg-10-5311-2013, 2013.
Krol, M., Houweling, S., Bregman, B., van den Broek, M., Segers, A., van Velthoven, P., Peters, W., Dentener, F., and Bergamaschi, P.: The two-way nested global chemistry-transport zoom model TM5: algorithm and applications, Atmos. Chem. Phys., 5, 417–432, doi:10.5194/acp-5-417-2005, 2005.
Le Quéré, C., Raupach, M. R., Canadell, J. G., and Marland, G.: Trends in the sources and sinks of carbon dioxide, Nat. Geosci., 2, 831–836, 2009.
Machida, T., Matsueda, H., Sawa, Y., Nakagawa, Y., Hirotani, K., Kondo, N., Goto, K., Nakazawa, T., Ishikawa, K., and Ogawa, T.: Worldwide measurements of atmospheric CO_2

ACPD
13, 27597–27639, 2013

and other trace gas species using commercial airlines, J. Atmos. Ocean. Tech., 25, 1744–1754, 2008.
Machida, T., Tohjima, Y., Katsumata, K., and Mukai, H.: A New CO_2 Calibration Scale Based on Gravimetric One-Step Dilution Cylinders in National Institute for Environmental Studies-NIES 09 CO_2 Scale, World Meteorol. Organ., Geneva, Switzerland, 114–119, 2011.
Maki, T., Ikegami, M., Fujita, T., Hirahara, T., Yamada, K., Mori, K., Takeuchi, A., Tsutsumi, Y., Suda, K., and Conway, T.: New technique to analyse global distributions of CO_2 concentrations and fluxes from non – processed observational data, Tellus B, 62, 797–809, 2010.
Maksyutov, S., Machida, T., Mukai, H., Patra, P. K., Nakazawa, T., and Inoue, G.: Effect of recent observations on Asian CO_2 flux estimates by transport model inversions, Tellus B, 55, 522–529, 2003.
Marland, G., Boden, T. A., Andres, R. J., Brenkert, A., and Johnston, C.: Global, Regional, and National Fossil Fuel CO_2 Emissions, Trends: a Compendium of Data on Global Change, Carbon Dioxide Information Analysis Center, Oak Ridge National Laboratory, http://cdiac.ornl.gov/trends/emis/overview, 2003.
Masarie, K., Pétron, G., Andrews, A., Bruhwiler, L., Conway, T., Jacobson, A., Miller, J., Tans, P., Worthy, D., and Peters, W.: Impact of CO_2 measurement bias on CarbonTracker surface flux estimates, J. Geophys. Res., 116, D17305, doi:10.1029/2011JD016270, 2011.
Matsueda, H., Machida, T., Sawa, Y., Nakagawa, Y., Hirotani, K., Ikeda, H., Kondo, N., and Goto, K.: Evaluation of atmospheric CO sub (2) measurements from new flask air sampling of JAL airliner observations, Pap. Meteorol. Geophys., 59, 1–17, 2008.
Mizoguchi, Y., Miyata, A., Ohtani, Y., Hirata, R., and Yuta, S.: A review of tower flux observation sites in Asia, J. Forest Res.-Jpn., 14, 1–9, 2009.
Mohammat, A., Wang, X., Xu, X., Peng, L., Yang, Y., Zhang, X., Myneni, R. B., and Piao, S.: Drought and spring cooling induced recent decrease in vegetation growth in Inner Asia, Agr. Forest Meteorol., 178–179, 21–30, 2012.
NationalClimateCenter: 2010 China Climate Bulletin, China Meteorological Press, 1–34, 2011.
Niwa, Y., Patra, P. K., Sawa, Y., Machida, T., Matsueda, H., Belikov, D., Maki, T., Ikegami, M., Imasu, R., Maksyutov, S., Oda, T., Satoh, M., and Takigawa, M.: Three-dimensional variations of atmospheric CO_2: aircraft measurements and multi-transport model simulations, Atmos. Chem. Phys., 11, 13359–13375, doi:10.5194/acp-11-13359-2011, 2011.
Niwa, Y., Machida, T., Sawa, Y., Matsueda, H., Schuck, T. J., Brenninkmeijer, C. A. M., Imasu, R., and Satoh, M.: Imposing strong constraints on tropical terrestrial CO_2 fluxes

ACPD
13, 27597–27639, 2013

Estimating Asian terrestrial carbon fluxes from CONTRAIL aircraft

H. F. Zhang et al.

using passenger aircraft based measurements, J. Geophys. Res.-Atmos., 117, D11303, doi:10.1029/2012JD017474, 2012.
Oikawa, T. and Ito, A.: Modeling Carbon Dynamics of Terrestrial Ecosystems in Monsoon Asia, Present and Future Modeling Global Environmental Change: Toward Integrated Modeling, TERRAPUB, Tokyo, 207–219, 2001.
Olivier, J. and Berdowski, J.: Global Emission Sources and Sinks, Lisse (the Netherlands): Balkema, 2001.
Olson, J. S., Watts, J. A., and Allison, L. J.: Major World Ecosystem Complexes Ranked by Carbon in Live Vegetation: A Database, NDP-017, Oak Ridge Lab., Oak Ridge, TN, 1985.
Pan, Y., Birdsey, R. A., Fang, J., Houghton, R., Kauppi, P. E., Kurz, W. A., Phillips, O. L., Shvidenko, A., Lewis, S. L., Canadell, J. G., Ciais, P., Jackson, R. B., Pacala, S. W., McGuire, A. D., Piao, S., Rautiainen, A., Sitch, S., and Hayes, D.: A large and persistent carbon sink in the world's forests, Science, 333, 988–993, 2011.
Patra, P. K., Niwa, Y., Schuck, T. J., Brenninkmeijer, C. A. M., Machida, T., Matsueda, H., and Sawa, Y.: Carbon balance of South Asia constrained by passenger aircraft CO_2 measurements, Atmos. Chem. Phys., 11, 4163–4175, doi:10.5194/acp-11-4163-2011, 2011.
Patra, P. K., Canadell, J. G., and Lal, S.: The rapidly changing greenhouse gas budget of Asia, Eos. T. Am. Geophys. Un., 93, 237–237, 2012.
Patra, P. K., Canadell, J. G., Houghton, R. A., Piao, S. L., Oh, N.-H., Ciais, P., Manjunath, K. R., Chhabra, A., Wang, T., Bhattacharya, T., Bousquet, P., Hartman, J., Ito, A., Mayorga, E., Niwa, Y., Raymond, P. A., Sarma, V. V. S. S., and Lasco, R.: The carbon budget of South Asia, Biogeosciences, 10, 513–527, doi:10.5194/bg-10-513-2013, 2013.
Peters, G. P., Marland, G., Le Quéré, C., Boden, T., Canadell, J. G., and Raupach, M. R.: Rapid growth in CO_2 emissions after the 2008–2009 global financial crisis, Nature Climate Change, 2, 2–4, 2011.
Peters, W., Jacobson, A. R., Sweeney, C., Andrews, A. E., Conway, T. J., Masarie, K., Miller, J. B., Bruhwiler, L. M. P., Petron, G., and Hirsch, A. I.: An atmospheric perspective on North American carbon dioxide exchange: CarbonTracker, P. Natl. Acad. Sci. USA, 104, 18925–18930, 2007.
Peters, W., Krol, M., Van der Werf, G., Houweling, S., Jones, C., Hughes, J., Schaefer, K., Masarie, K., Jacobson, A., and Miller, J.: Seven years of recent European net terrestrial carbon dioxide exchange constrained by atmospheric observations, Glob. Change Biol., 16, 1317–1337, 2010.

Peylin, P., Rayner, P. J., Bousquet, P., Carouge, C., Hourdin, F., Heinrich, P., Ciais, P., and AEROCARB contributors: Daily CO_2 flux estimates over Europe from continuous atmospheric measurements: 1, inverse methodology, Atmos. Chem. Phys., 5, 3173–3186, doi:10.5194/acp-5-3173-2005, 2005.
Peylin, P., Law, R. M., Gurney, K. R., Chevallier, F., Jacobson, A. R., Maki, T., Niwa, Y., Patra, P. K., Peters, W., Rayner, P. J., Rödenbeck, C., and Zhang, X.: Global atmospheric carbon budget: results from an ensemble of atmospheric CO_2 inversions, Biogeosciences Discuss., 10, 5301–5360, doi:10.5194/bgd-10-5301-2013, 2013.
Piao, S., Fang, J., Ciais, P., Peylin, P., Huang, Y., Sitch, S., and Wang, T.: The carbon balance of terrestrial ecosystems in China, Nature, 458, 1009–1013, 2009.
Piao, S. L., Ciais, P., Lomas, M., Beer, C., Liu, H. Y., Fang, J. Y., Friedlingstein, P., Huang, Y., Muraoka, H., Son, Y. H., and Woodward, I.: Contribution of climate change and rising CO_2 to terrestrial carbon balance in East Asia: a multi-model analysis, Global Planet. Change, 75, 133–142, 2011.
Piao, S. L., Ito, A., Li, S. G., Huang, Y., Ciais, P., Wang, X. H., Peng, S. S., Nan, H. J., Zhao, C., Ahlström, A., Andres, R. J., Chevallier, F., Fang, J. Y., Hartmann, J., Huntingford, C., Jeong, S., Levis, S., Levy, P. E., Li, J. S., Lomas, M. R., Mao, J. F., Mayorga, E., Mohammat, A., Muraoka, H., Peng, C. H., Peylin, P., Poulter, B., Shen, Z. H., Shi, X., Sitch, S., Tao, S., Tian, H. Q., Wu, X. P., Xu, M., Yu, G. R., Viovy, N., Zaehle, S., Zeng, N., and Zhu, B.: The carbon budget of terrestrial ecosystems in East Asia over the last two decades, Biogeosciences, 9, 3571–3586, doi:10.5194/bg-9-3571-2012, 2012.
Randall, D. A., Dazlich, D. A., Zhang, C., Denning, A. S., Sellers, P. J., Tucker, C. J., Bounoua, L., Los, S. O., Justice, C. O., and Fung, I.: A revised land surface parameterization (SiB2) for GCMs. 3. The greening of the Colorado State University general circulation model, J. Climate, 9, 738–763, 1996.
Randerson, J. T., Thompson, M. V., Conway, T. J., Fung, I. Y., and Field, C. B.: The contribution of terrestrial sources and sinks to trends in the seasonal cycle of atmospheric carbon dioxide, Global Biogeochem. Cy., 11, 535–560, 1997.
Raupach, M. R., Marland, G., Ciais, P., Le Quéré, C., Canadell, J. G., Klepper, G., and Field, C. B.: Global and regional drivers of accelerating CO_2 emissions, P. Natl. Acad. Sci. USA, 104, 10288–10293, 2007.

ACPD
13, 27597–27639, 2013

Richardson, A. D., Hollinger, D. Y., Dail, D. B., Lee, J. T., Munger, J. W., and O'Keefe, J.: Influence of spring phenology on seasonal and annual carbon balance in two contrasting New England forests, Tree Physiol., 29, 321–331, 2009.

Rivier, L., Peylin, P., Ciais, P., Gloor, M., Rödenbeck, C., Geels, C., Karstens, U., Bousquet, P., Brandt, J., and Heimann, M.: European CO_2 fluxes from atmospheric inversions using regional and global transport models, Climatic Change, 103, 93–115, 2010.

Rivier, L., Peylin, P., Ciais, P., Gloor, M., Rödenbeck, C., Geels, C., Karstens, U., Bousquet, P., Brandt, J., and Heimann, M.: European CO_2 fluxes from atmospheric inversions using regional and global transport models, in: Greenhouse Gas Inventories, Springer, 2011.

Saeki, T., Maksyutov, S., Sasakawa, M., Machida, T., Arshinov, M., Tans, P., Conway, T., Saito, M., Valsala, V., and Oda, T.: Carbon flux estimation for Siberia by inverse modeling constrained by aircraft and tower CO_2 measurements, J. Geophys. Res.-Atmos., 118, 1100–1122, 2013.

Sawa, Y., Machida, T., and Matsueda, H.: Seasonal variations of CO_2 near the tropopause observed by commercial aircraft, J. Geophys. Res., 113, D23301, doi:10.1029/2008JD010568, 2008.

Scurlock, J. and Hall, D.: The global carbon sink: a grassland perspective, Glob. Change Biol., 4, 229–233, 1998.

Sellers, P., Mintz, Y., Sud, Y., and Dalcher, A.: A simple biosphere model (SiB) for use within general circulation models, J. Atmos. Sci., 43, 505–531, 1986.

Sellers, P., Randall, D., Collatz, G., Berry, J., Field, C., Dazlich, D., Zhang, C., Collelo, G., and Bounoua, L.: A revised land surface parameterization (SiB2) for atmospheric GCMs. Part I: Model formulation, J. Climate, 9, 676–705, 1996.

Stephens, B. B., Gurney, K. R., Tans, P. P., Sweeney, C., Peters, W., Bruhwiler, L., Ciais, P., Ramonet, M., Bousquet, P., and Nakazawa, T.: Weak northern and strong tropical land carbon uptake from vertical profiles of atmospheric CO_2, Science, 316, 1732–1735, 2007.

Takahashi, T., Wanninkhof, R., Feely, R., Weiss, R., Chipman, D., Bates, N., Olafsson, J., Sabine, C., and Sutherland, S.: Net Sea-Air CO_2 Flux Over the Global Oceans: an Improved Estimate Based on the Sea-Air pCO_2 Difference, Proceedings of the 2nd International Symposium CO_2 in the Oceans, Tsukuba, Japan: National Institute for Environmental Studies, 1999.

Thoning, K. W., Tans, P. P., and Komhyr, W. D.: Atmospheric carbon dioxide at Mauna Loa Observatory: 2. analysis of the NOAA GMCC data, 1974–1985, J. Geophys. Res.-Atmos., 94, 8549–8565, 1989.
Tian, H., Melillo, J., Lu, C., Kicklighter, D., Liu, M., Ren, W., Xu, X., Chen, G., Zhang, C., and Pan, S.: China's terrestrial carbon balance: contributions from multiple global change factors, Global Biogeochem. Cy., 25, GB1007, doi:10.1029/2010GB003838, 2011.
Valsala, V., Tiwari, Y. K., Pillai, P., Roxy, M., Maksyutov, S., and Murtugudde, R.: Intraseasonal variability of terrestrial biospheric CO_2 fluxes over India during summer monsoons, J. Geophys. Res.-Biogeo., 118, 752–769, 2013.
van der Werf, G. R., Randerson, J. T., Giglio, L., Collatz, G. J., Kasibhatla, P. S., and Arellano Jr., A. F.: Interannual variability in global biomass burning emissions from 1997 to 2004, Atmos. Chem. Phys., 6, 3423–3441, doi:10.5194/acp-6-3423-2006, 2006.
Walther, G.-R., Post, E., Convey, P., Menzel, A., Parmesan, C., Beebee, T. J., Fromentin, J.-M., Hoegh-Guldberg, O., and Bairlein, F.: Ecological responses to recent climate change, Nature, 416, 389–395, 2002.
Wang, H., Zhang, R., Liu, M., and Bi, J.: The carbon emissions of Chinese cities, Atmos. Chem. Phys., 12, 6197–6206, doi:10.5194/acp-12-6197-2012, 2012.
Wang, X., Piao, S., Ciais, P., Li, J., Friedlingstein, P., Koven, C., and Chen, A.: Spring temperature change and its implication in the change of vegetation growth in North America from 1982 to 2006, P. Natl. Acad. Sci. USA, 108, 1240–1245, 2011.
Yang, Z., Washenfelder, R., Keppel-Aleks, G., Krakauer, N., Randerson, J., Tans, P., Sweeney, C., and Wennberg, P.: New constraints on Northern Hemisphere growing season net flux, Geophys. Res. Lett., 34, L12807, doi:10.1029/2007GL029742, 2007.
Yu, G. R., Zhu, X. J., Fu, Y. L., He, H. L., Wang, Q. F., Wen, X. F., Li, X. R., Zhang, L. M., Zhang, L., and Su, W.: Spatial patterns and climate drivers of carbon fluxes in terrestrial ecosystems of China, Glob. Change Biol., 19, 798–810, 2013.

ACPD
13, 27597–27639, 2013

ACPD
13, 27597–27639, 2013

Table 1. Summary of the Asian surface CO_2 observation data assimilated between 1 January 2006 and 31 December 2010. The frequency of continuous data is one per day (when available), while discrete surface data is generally once per week. MDM (model-data-mismatch) is a value assigned to a given site that is meant to quantify our expected ability to simulate observations and used to calculate the innovation X^2 (Inn. X^2) statistic. N denotes that the number is available in the CTDAS. Flagged observations mean a model-minus-observation difference that exceeds 3 times of the model-data-mismatch and are therefore excluded from assimilation. The bias is the average from posterior residuals (final modeled values – measured values).

Site	Name	Lat., Lon., Elev.	Lab	N (flagged)	MDM	Inn. X^2	Bias
Discrete samples:							
WLG	Waliguan, China	36.29° N, 100.90° E, 3810 m	CMA/ESRL	254(19)	1.5	0.83	−0.10
BKT	Bukit Kototabang, Indonesia	0.20° S, 100.312° E, 864 m	ESRL	172(0)	7.5	0.73	5.53
WIS	Sede Boker, Israel	31.13° N, 34.88° E, 400 m	ESRL	239(1)	2.5	0.62	−0.10
KZD	Sary Taukum, Kazakhstan	44.45° N, 77.57° E, 412 m	ESRL	167(6)	2.5	1.16	−0.08
KZM	Plateau Assy, Kazakhstan	43.25° N, 77.88° E, 2519 m	ESRL	155(2)	2.5	0.96	0.50
TAP	Tae-ahn Peninsula, Korea	36.73° N, 126.13° E, 20 m	ESRL	181(3)	7.5	0.60	1.82
UUM	Ulaan Uul, Mongolia	44.45° N, 111.10° E, 914 m	ESRL	231(5)	2.5	1.17	0.10
CRI	Cape Rama, India	15.08° N, 73.83° E, 60 m	CSIRO	33(1)	3	1.40	−1.97
LLN	Lulin, China	23.47° N, 120.87° E, 2867 m	ESRL	220(20)	7.5	0.99	2.62
SDZ	Shangdianzi, China	40.39° N, 117.07° E, 287 m	CMA/ESRL	60(15)	3	1.18	0.15
Continuous samples:							
MNM	Minamitorishima, Japan	24.29° N, 153.98° E, 8 m	JMA	1624(0)	3	0.76	0.15
RYO	Ryori, Japan	39.03° N, 141.82° E, 260 m	JMA	1663(48)	3	0.90	0.46
YON	Yonagunijima, Japan	24.47° N, 123.02° E, 30 m	JMA	1684(3)	3	0.78	1.53
GSN	Gosan, Republic of Korea	33.15° N, 126.12° E, 72 m	NIER	1274(39)	3	1.99	−1.01

Table 2. Summary of the Asian CONTRAIL CO_2 observation data assimilated between 2006 and 2010. MDM (model-data-mismatch) is a value assigned to a given site that is meant to quantify our expected ability to simulate observations and used to calculate the innovation X^2 (Inn. X^2) statistic. N denotes that the number is available in the CTDAS. Flagged observations mean a model-minus-observation difference that exceeds 3 times of the model-data-mismatch and are therefore excluded from assimilation. The bias is the average from posterior residuals (final modeled values – measured values).

Pressure Level	N (flagged)	MDM	Inn. X^2	Bias
575–625 hPa	0	2.00	0.00	0.00
485–525 hPa	2907(5)	2.00	0.35	0.05
375–425 hPa	3035(3)	2.00	0.34	0.05
225–275 hPa	4525(4)	2.00	0.34	0.04

ACPD
13, 27597–27639, 2013

Table 3. Results of the sensitivity experiments conducted in this study ($Pg\,C\,yr^{-1}$).

Case 1	Case 2	Case 3	Case 4	Case 5	Case 6
−1.56	−1.09	−1.69	−1.80	−1.23	−1.07

The Case 1 (with CONTRAIL) and Case 2 (without CONTRAIL) run for the period 2006–2010, while Case 3–6 run for the period 2008–2010.

ACPD
13, 27597–27639, 2013

Table 4. Terrestrial biosphere fluxes considered in ecosystem types for 2006–2010 ($Pg\,C\,yr^{-1}$).

	Type	Asia	Boreal Eurasia	Temperate Eurasia	Tropical Asia	Asia	Boreal Eurasia	Temperate Eurasia	Tropical Asia
Forest	Conifer Forest	−0.64	−0.63	−0.02	0.00	−0.77	−0.71	−0.11	+0.04
	Broadleaf Forest	−0.04	−0.01	−0.01	−0.01				
	Mixed Forest	−0.14	−0.05	−0.07	−0.03				
	Fields/Woods/Savanna	−0.01	−0.01	0.00	0.00				
	Forest/Field	−0.02	−0.01	−0.01	0.00				
	Tropical Forest	+0.08	0.00	0.00	+0.08				
Grass/Shrub	Grass/Shrub	−0.43	−0.06	−0.36	−0.02	−0.44	−0.06	−0.36	−0.02
	Scrub/Woods	0.00	0.00	0.00	0.00				
	Shrub/Tree/Suc.	0.00	0.00	0.00	0.00				
crop	Crops	−0.20	−0.02	−0.17	−0.01	−0.20	−0.02	−0.17	−0.01
others	Semitundra	−0.09	−0.05	−0.04	0.00	−0.15	−0.23	−0.04	+0.13
	Northern Taiga	−0.17	−0.17	0.00	0.00				
	Wooded tundra	0.00	0.00	0.00	+0.06				
	Mangrove	0.00	0.00	0.00	0.00				
	Non-optimized	0.00	0.00	0.00	0.00				
	Water	0.07	0.00	0.00	+0.07				
	Wetland	+0.04	−0.01	0.00	0.00				
	Deserts	0.00	0.00	0.00	0.00				

ACPD
13, 27597–27639, 2013

Table 5. The inverted flux magnitudes and Gaussian error reduction rate between surface-only and surface-CONTRAIL during 2006–2010 ($Pg\,C\,yr^{-1}$).

Region	flux			Gaussian error		
	Surface-only	Surface-CONTRAIL	Flux difference	Surface-only	Surface-CONTRAIL	Error reduction (%)
Boreal Eurasia	−0.96	−1.02	−0.06	1.05	0.91	14
Temperate Eurasia	−0.33	−0.68	−0.35	0.75	0.70	6
Tropical Asia	+0.19	+0.15	−0.05	0.33	0.28	15
Asia	−1.09	−1.56	−0.47	1.34	1.18	11

ACPD
13, 27597–27639, 2013

Table 6. Comparison of the inverted carbon sinks in this study with previous studies (Pg C yr^{-1}).

Reference	Period	Boreal Eurasia	Temperate Eurasia	Tropical Asia	Asia	Remarks
This study	2006–2010	−1.02 ± 0.91	−0.68 ± 0.70	+0.14 ± 0.28	−1.56 ± 1.18	surface-CONTRAIL
Gurney et al. (2003)	1992–1996	−0.59 ± 0.52	−0.60 ± 0.67	+0.67 ± 0.70	−0.52 ± 0.65	–
Maki et al. (2010)	2001–2007	−1.46 ± 0.41	0.96 ± 0.59	−0.15 ± 0.44	−0.65 ± 0.49	CNTL experiments
		−1.38 ± 0.42	0.37 ± 0.62	−0.16 ± 0.45	−1.17 ± 0.50	OBS experiments
Piao et al. (2012)[a]	1990–2009	–	−0.38 ± 0.50	–	–	Focused on East Asia
Niwa et al. (2012)[b]	2006–2008	−0.34 ± 0.23	−0.05 ± 0.27	+0.45 ± 0.19	+0.06 ± 0.40	GVCT
		−0.25 ± 0.28	−0.32 ± 0.32	+0.03 ± 0.29	−0.54 ± 0.51	GV
Patra et al. (2013)[c]	2007–2008	–	–	−0.104 ± 0.15	–	Focused on South Asia

[a] East Asia, a region comprised of China, Japan, North- and South-Korea, and Mongolia.
[b] GVCT: together use GLOBALVIEW and CONTRAIL CO_2 observation data to perform inversion. GV: only use GLOBALVIEW data to conduct inversion.
[c] South Asia, a region comprised of Bangladesh, Bhutan, India, Nepal, Pakistan and Sri Lanka.

ACPD
13, 27597–27639, 2013

Estimating Asian terrestrial carbon fluxes from CONTRAIL aircraft

H. F. Zhang et al.

Discussion Paper | Discussion Paper | Discussion Paper | Discussion Paper |

ACPD
13, 27597–27639, 2013

Estimating Asian terrestrial carbon fluxes from CONTRAIL aircraft

H. F. Zhang et al.

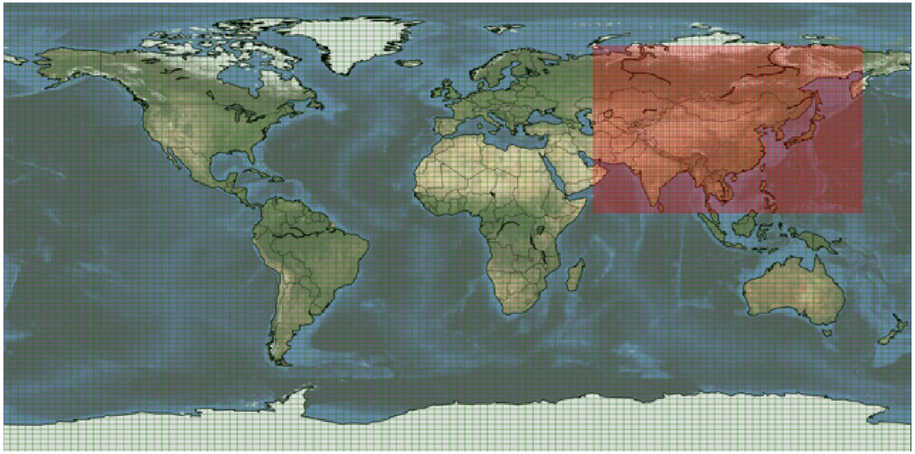

Fig. 1. TM5 global grid (3 × 2) with zoom over Asia (1 × 1).

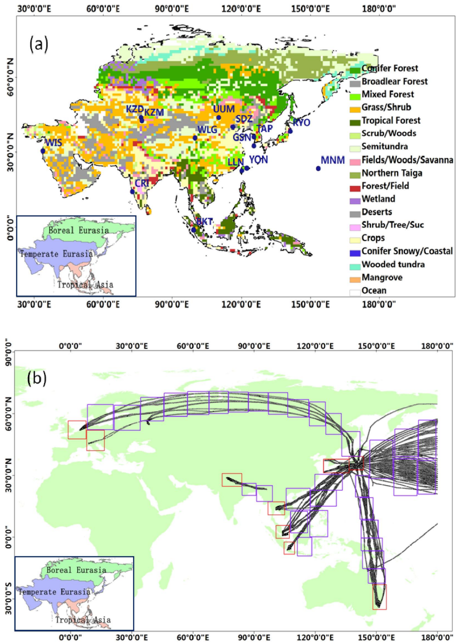

Fig. 2. (a) Map of the Asian surface observation sites, along with the map of the ecoregion types from Olson et al. (1985) with 19 land cover classes as used in this study. A map of the global surface observation sites from the NOAA-ESRL, CSIRO and WDCGG network are in the **(a)**; **(b)** Asian CONTRAIL CO_2 observations map, along with 42 horizontal regions. The red rectangles represent the 9 regions covering the ascending and descending data (included 4 vertical bins at 575–625, 475–525, 375–425, 225–275 hPa) over airports, and the blue rectangles indicate the other 33 regions covering the cruise data (included 1 bin at 225–275 hPa). Note that "Asia" refers to lands as far west as the Urals in this study and it is further divided into Boreal Eurasia, Temperate Eurasia and tropical Asia based on TransCom regions (Gurney et al., 2002; Gurney et al., 2003). These divided regions are presented in the small inset in the bottom left corner (same as thereafter).

ACPD
13, 27597–27639, 2013

Estimating Asian terrestrial carbon fluxes from CONTRAIL aircraft

H. F. Zhang et al.

Title Page
Abstract Introduction
Conclusions References
Tables Figures
◀ ▶
Back Close
Full Screen / Esc
Printer-friendly Version
Interactive Discussion

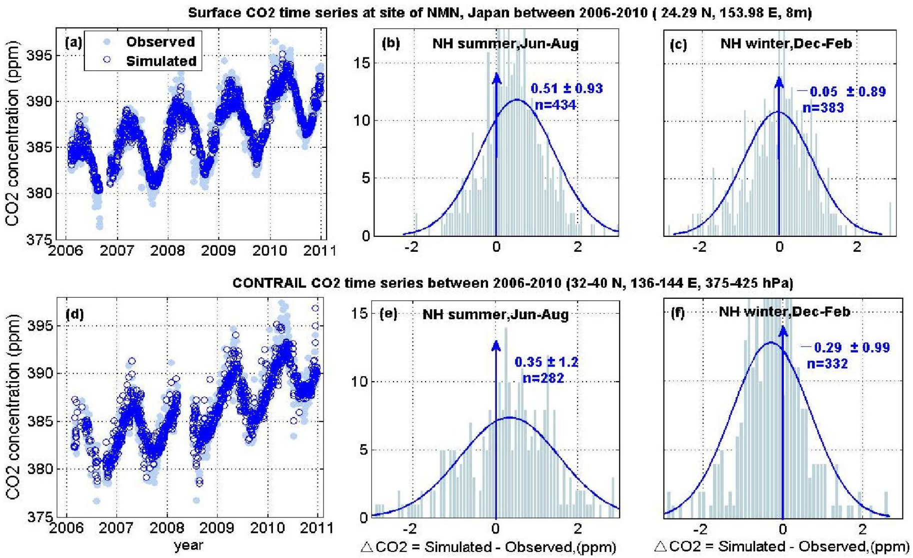

Fig. 3. (a) CO_2 observed and simulated time series; **(b)** summer histograms of the residuals (residuals = simulated-minus-observed); **(c)** winter histograms of the residuals at Surface site of NMN during 2006–2010. **(d)** CO_2 observed and simulated time series; **(e)** summer histograms of the residuals (residuals = simulated-minus-observed); **(f)** winter histograms of the residuals of CONTRAIL CO_2 during the period 2006–2010 in the region covering 136–144° N, 32–40° E, 375–425 hPa. The blue column in (**b**, **c**, **e** and **f**) shows the histogram of the residuals themselves, and the blue lines and statistics shown in blue text (indicated mean, standard deviation and observed number, respectively) are a summary of the residuals interpreted as a normal distribution. The vertical scales are determined by the number of observations and how tightly they are grouped, with the area under the histogram forced to unity.

ACPD
13, 27597–27639, 2013

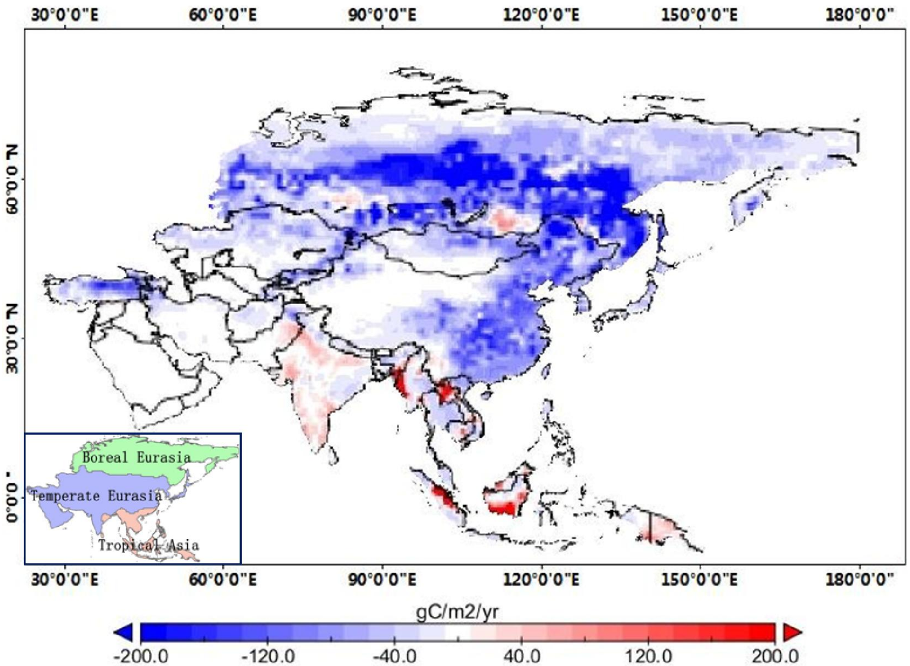

Fig. 4. Mean terrestrial biosphere carbon flux estimated from our system over Asia during 2006–2010 at a 1 × 1 grid. Blue colors (negative) denote net carbon uptake while red colors (positive) denote carbon release to the atmosphere. Note that the estimated flux map includes net terrestrial fluxes and biomass burning sources but excludes fossil fuel emissions.

ACPD
13, 27597–27639, 2013

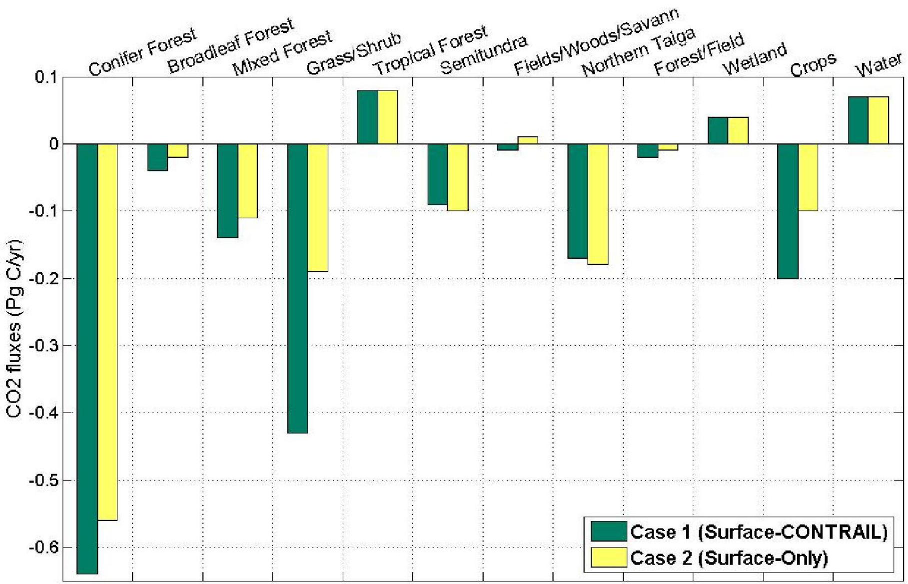

Fig. 5. Fluxes per ecoregion in Asia averaged over the period 2006–2010 in Case 1 and Case 2 ($Pg\,C\,yr^{-1}$).

ACPD
13, 27597–27639, 2013

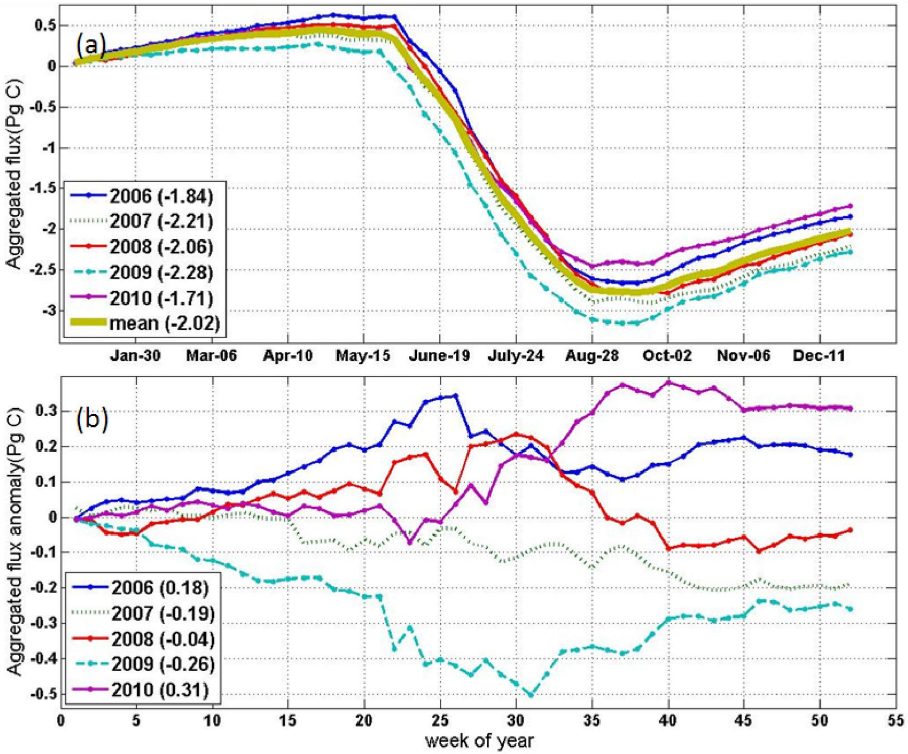

Fig. 6. (a) Cumulative net ecosystem exchange (NEE) vs. time estimated in our system for each of the individual years and for the 2006–2010 mean. This figure reveals the largest uptake in 2009 and the smallest uptake in 2010. **(b)** Cumulative anomaly of CO_2 exchange through the year 2006–2010. The fluxes shown here include only respiration and photosynthesis, because the biomass burning emissions have a large inter-annual variability.

ACPD
13, 27597–27639, 2013

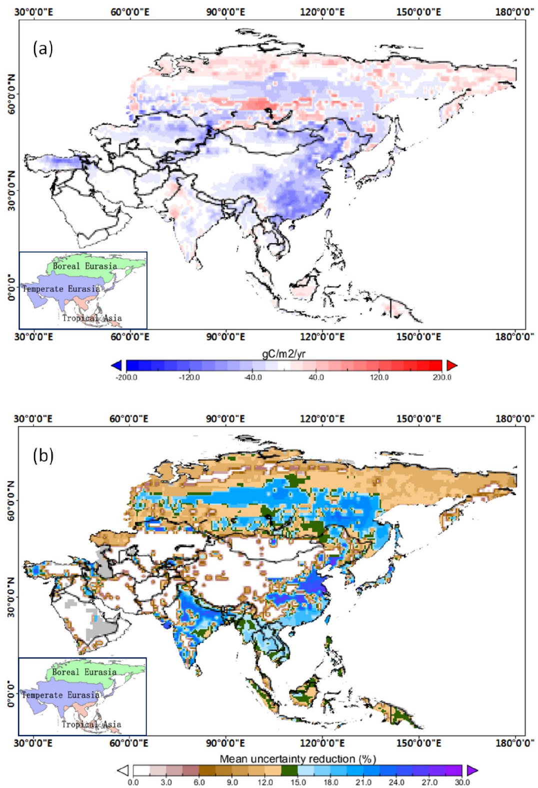

Fig. 7. (a) The inverted flux difference between surface CO_2 observation data only surface (surface-only) and both the surface CO_2 observation data and CONTRAIL data (surface-CONTRAIL); and **(b)** the Gaussian error reduction rate between surface-only and surface-CONTRAIL during 2006–2010. The flux difference is derived from: (surface-CONTRAIL – surface-only), while the Gaussian error reduction rate is calculated as: $(\sigma_{\text{surface-only}} - \sigma_{\text{surface-CONTRAIL}})/\sigma_{\text{surface-only}} \times 100$.

ACPD
13, 27597–27639, 2013

Title Page
Abstract | Introduction
Conclusions | References
Tables | Figures
◀◀ | ▶▶
◀ | ▶
Back | Close
Full Screen / Esc
Printer-friendly Version
Interactive Discussion